Polarization-independent wideband meta-material rasorber with wide transmission window based on resistor loaded circular and split ring resonators

Abhinav Kumar[1,3], Gobinda Sen[2] and Jayanta Ghosh[3]
[1]ECE Dept., Bhagalpur college of Engineering, Bihar, India
[2]ECE Dept.,Institute of Engineering and Management, Kolkta, India
[3]ECE Dept., National Institute of Technology, Patna

Corresponding author: Abhinav Kumar (abhinavk.phd19.ece@nitp.ac.in)

ABSTRACT A dual polarized with high absorption to right side and wide in-band transmission is proposed in this study. Our proposed design consists of four modified split ring resonators on the top layer and four lumped resistor of 150 Ω value is connected between them to absorb the incoming EM wave in the out-of-band frequency regime.The circular slotted cut on the lower layer is responsible for in-band transmission. The lower layer is behaving as a ground plane for out-of-band absorption and and passing a range of frequency for the transmission band. So, bottom layer is behave as a band-pass frequency selective surface filter. The design has an overall thickness of 0.18λ and a fractional bandwidth of approximately 113%. The entire design exhibits an insertion loss of 1.10 dB at the transmission band at around 5.93 GHz and exceeding 80% absorption from 2.8 GHz to 10.0 GHz. The proposed design is polarization insensitive due to its symmetrical design and angularly stable up to 45° for both both TE and TM polarization of wave.
The novelty of the proposed design lies in its wide out-of-band absorption, wide in-band transmission, minimal thickness, high fractional bandwidth, good angular stability, cost-effectiveness, accessibility through the use of inexpensive materials for manufacture and simple design. To analyze the proposed rasorber, we have investigated the polarization behavior, surface current distribution and design other parameters. Lastly, the proposed structure has been constructed using PCB technology and validated in a semi-anechoic chamber. The simulated and measured responses exhibit a high degree of agreement.

INDEX TERMS Band-pass filter; Frequency selective surface; Microwave absorber; Radar cross-section; Radomes; A-T-A(Absorption-Transmission-Absorption)

I. INTRODUCTION

RASORBER selectively blocks or absorbs the majority of the incident radiation, while allowing a range of frequencies to transmit with little attenuation. It generally consists of two-layer structures. The top layer is responsible for out-of-band absorption while the bottom layer is designed to function as a band-pass filter to pass the in-band EM wave. The top layer is included with different absorption techniques and mechanisms to absorb the out-of-band EM wave while the bottom layer behaves as a ground plane for the out-of-band absorption and passes the transmission window. It creates a shield around the object to reduce the possibility of detection by radar but passing the desired band for some purpose. As a result, they are transparent for in-band signals and opaque for out-of-band signals. It is employed in military aircraft and ships to safeguard them from hostile radar. To lessen the chance of mishaps brought on by collisions with other objects, they can also be utilized in recreational vehicles like boats and autos [1]. To minimize the radar cross section (RCS), improve radiation performance, and prevent mutual interference, FSSs have been used extensively as hybrid radomes for antenna systems [2], [3], [4], [5]. These are called rasorbers because they are employed in radome-based structures [6], [7]. Radomes are constructed using materials that reflect or block signals in the radio frequency range, rendering them difficult for radar to detect. The radome's shape can also be configured to reduce the quantity of radiation emitted by the structure [8]. Today, radomes are receiving increased attention as a result of their ability to absorb out-of-band signals and transmit in-band signals. Radomes consist of two layers out of which one layer is used for transmission and the other layer for absorption. The top layer is design to absorb the EM wave in a wide frequency range. Researchers over the world has employed different techniques to increase the absorption bandwidth of the structure. Multi-resonant structures are implemented to

achieve wideband absorption; a combination of resonators tuned to various frequencies can be used. Multiple absorption peaks are possible with this approach and collectively span a wide frequency range [9]; [10]. Better impedance matching over a wide frequency range is made possible by gradient-index metamaterials, which gradually switch from one impedance to another. The bandwidth of metamaterial absorbers (MMAs) can be greatly increased using this design approach [11]; [12]. To increase the absorption bandwidth, the thickness of the dielectric substrate supports should be increased. However, the larger absorber's total size is the trade-off. An important trade-off in the wideband MMA design is optimizing thickness [13]. Using resistive materials such as resistive sheets, lump resistors, and resistive inks [14]; [15]; [16]; [17], FSS-based microwave absorbers can be designed to absorb a broad spectrum of frequencies.

A band-pass selective transmission can be designed by cutting different slot design in the lower stratum [18]. These two frequency-selective surface structures are maintained by an air separation or another distinct material to serve as a transmission window between two absorption bands. Rasorbers are hybrid of a filter and an absorber. The transmission band was initially observed before the absorption band, with the band-pass geometry arranged beneath the resistive sheet [19]. The design of a rasorber with an absorption band below the pass-band is a difficult endeavour due to the lossy property of sheets. These concerns have been addressed by the implementation of parallel *LC* design or dipole arrays, which elicit parallel resonance and produce a transmission band that follows the absorption band [20]. However, the signal of any one side of the pass band can only be absorbed by these two techniques. The rasorber with in-band communication is necessary to absorb the signal on both sides of the pass-band. This refers to the transmission window between two absorption bands on either side.

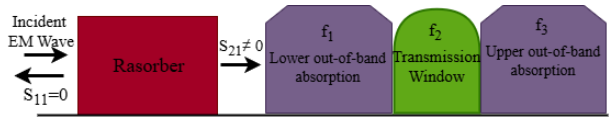

FIGURE 1: Absorption and transmission response of the Rasorber.

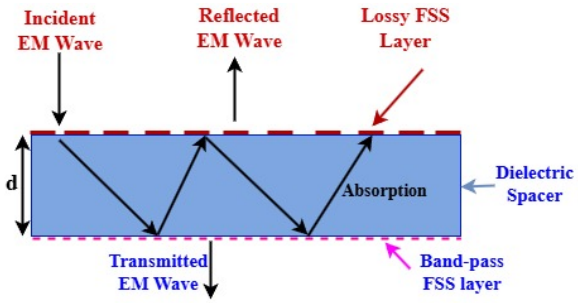

FIGURE 2: Absorption and transmission phenomena of the Rasorber based on parallel plate waveguide.

In this study, a polarization insensitive, high angle independent, wide out-of-band and wide transmission band has been designed, fabricated and experimentally measured using VNA. Rasorbers are a unique type of FSS that can simultaneously transmit a specific frequency band and absorb incoming signals.

The proposed design is composed of two layers; the resonator of the top layer consists of four split ring resonators and a chip resistor embedded between them. To pass the in-band signal a circular slot is cut from the copper in the lower layer. The circular slot design at the lower layer is responsible for the transmission band at 5.93 GHz, with a low insertion loss of approximately 1.1 dB. Meanwhile, the upper layer is laden with chip resistors to increase the bandwidth of the out-of-band absorption from 2.8 to 10.0 GHz. The proposed design's novelties include a wide transmission window, high fractional bandwidth, minimal thickness, affordability, accessibility due to the use of low-cost manufacturing materials, polarization insensitivity, angular stability, and simple design. The proposed rasorber has been investigated regarding angular stability, polarisation insensitivity, and design parameters. Ultimately, the simulated and measured results were compared and determined to be in excellent agreement.

II. THEORETICAL BACKGROUND

Rasorber generally comprises of two layers.

The upper layer is responsible for absorption of the signal and bottom layer will be act as ground plane for the absorption phenomena and transmit some particular frequency for the in-band operation. For, an ideal absorber the reflection coefficient $(S_{11} = 0)$ and transmission coefficient $(S_{21} = 0)$ should be zero to get optimum value of absorption, which can be evaluated from equation(1) [21].

$$A(\omega) = 1 - |S_{11}|^2 - |S_{21}|^2 \tag{1}$$

Where A(ω), $|S_{11}|^2$, $|S_{21}|^2$ is absorption, reflected power and transmitted power respectively. But the rasorber phenomena are different from absorber as shown in **Figure 1**

the overall frequency regime of the rasorber can be divided into three parts i.e. lower absorption band (f_1), transmission window (f_2) and upper absorption band (f_3).

For an ideal rasorber at f_1 and f_3, $S_{11} = 0$, $S_{21} = 0$ should be zero and at f_2, S_{21} should be unity. To get these phenomena, we have smartly design the rasorber as shown in **Figure 2** i.e. when impedance of the upper layer is matched to the free space impedance and zero for the lower layer, the structure behaves as absorber. To get transmission window the impedance of the both layers should be infinity.

III. UNIT CELL GEOMETRY

The proposed rasorber is composed of two layers in its unit cell geometry. The concept of a quarter-wave transmission line terminated with a brief circuit was employed in this design.

Therefore, it operates as a parallel resonant circuit, resulting in an infinite impedance when it resonates. To achieve this structure, we first devise a short-circuit quarter-wave

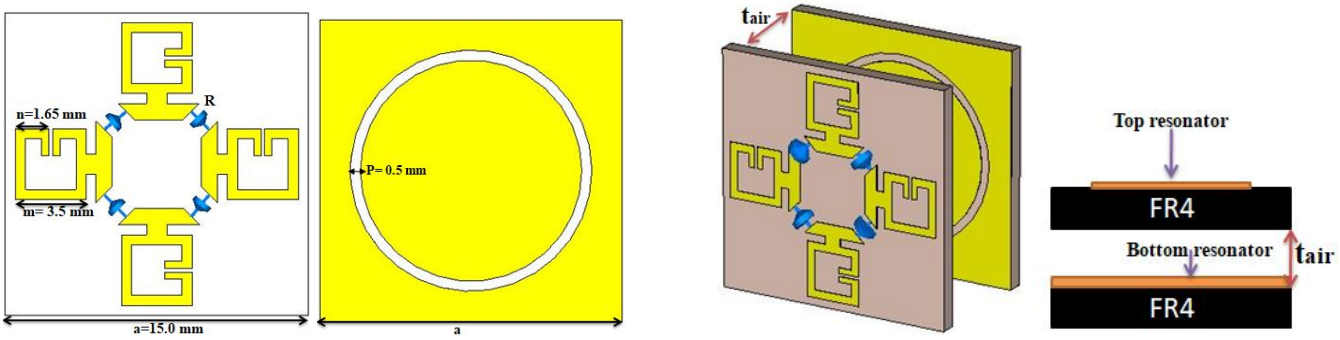

FIGURE 3: Schematic of the proposed unit cell Rasorber (a) Top layer (b) Bottom layer (c) Isometric view (d) Side view.

transmission line that is repeated in all four directions to achieve polarization-insensitive behaviour. The parallel $L_1 - C_1$ circuit is implemented by a modified split ring resonator located on a FR4 substrate. The finger of the split ring functions as an inductor, while the coupling between the fingers functions as a capacitor parallel to the inductor. The *R-L* series circuit is achieved by incorporating four chip resistors between the modified split ring resonator to achieve a reflection coefficient of less than -10 dB in the out-of-band absorption. After the top layer is completed, the lower layer must be designed to resonate at the same frequency as the transmission window and function as a ground plane for the out-of-band absorption. To achieve this, a parallel $L_2 - C_2$ resonator is implemented by incorporating a circular slit into a 1.0 mm FR4 substrate. The foam, which has a refractive index that is nearly equal to that of air, separates the upper and bottom layers. **Figure 3** illustrates the side and the isometric view of the proposed rasorber.

Chip resistors (R = 150 Ω) have been affixed to the FR4 substrate on the top layer, with a dielectric loss tangent and permittivity of 0.02 and 4.4, respectively. This will function as a lossy layer, facilitating the attainment of optimal out-of-band absorption. Because of this, the wideband absorption will be the responsibility of the upper layer. The in-band transmission window and out-of-band absorption are achieved by intelligently adjusting the air-gap. The optimal parameter of the proposed rasorber is as follows: *a=15 mm*, *m=3.5 mm*, *n=1.65 mm*, *p=0.5 mm*, *R =150* Ω, t_{air}*= 7.0 mm.*

IV. DESIGN EVOLUTION

The proposed rasorber comprises two layers. The upper layer is engineered to incorporate lumped element losses inside the structure; nonetheless, absorption is minimal on both sides of the transmission window, while in-band transmission is rather effective. The circular aperture in the lower layer facilitates in-band transmission, with minimal losses attributed to the finite loss tangent of the FR4 dielectric employed in the lower layer design. When the two layers are properly spaced, the lower layer functions as the ground plane for out-of-band absorption, hence improving total out-of-band absorption, as depicted in **Figure 4.**

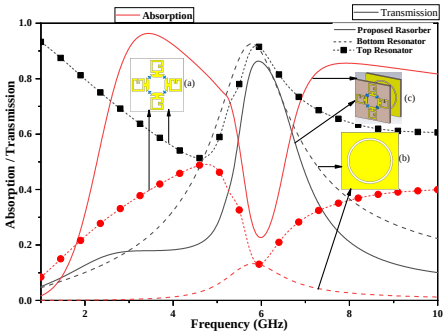

FIGURE 4: Design evolution of the Proposed Rasorber (a) Top resonator (b) Bottom resonator (c) Proposed Rasorber.

V. PARAMETRIC STUDY

To achieve the best possible result,a comprehensive parametric analysis is performed to optimize the various structural dimensions.

A. EFFECT OF DISTANCE BETWEEN THE UPPER AND BOTTOM RESONATOR

The air gap between the top and bottom layer is adjusted in such a way that the bottom layer behaves as a bandpass selective FSS filter, which passes the in-band transmission window while behaves as a ground plane for the out-of-band frequency regime. For the out-of-band operation, EM waves pass through the upper layer and reach to bottom layer which act as a ground plane and when the signal is reflected from the bottom layer, it becomes again reflected from the top layer as shown in **Figure 2** and this phenomena occur repeatedly to trap the EM waves inside the rasorber, if some signal leaks from the top layer, the air-gap between the top and bottom layer adjusted to $\frac{1}{4}$ wavelength of the absorption frequency to get destructive interference with the incoming signal at the surface of the top layer of the proposed rasorber. In the transmission window, the bottom layer resonates at the same frequency as the upper layer to pass the in-band signal with

low insertion loss. To obtain the above-mentioned design, we have adjusted the air gap between the upper and lower layers (t_{air}) from 6.0 to 8.0 mm. The optimal transmission and reflection coefficient found at t_{air} =7.0 mm is shown in **Figure 5**.

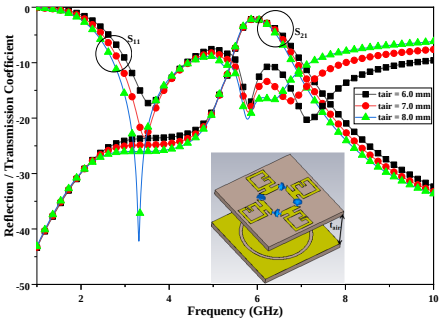

FIGURE 5: Reflection and transmission coefficient of the Proposed Rasorber for different values of air-gap between top and bottom FSS.

B. EFFECT OF CHIP RESISTOR

The chip resistors are responsible for wideband absorption in the out-of-band frequency regime. The upper layer is realized by a parallel $L_1 - C_1$ resonant circuit in series with a $R - L$ circuit. At the in-band frequency regime (i.e. transmission window) parallel $L_1 - C_1$ circuit resonant, it leads to infinity impedance of the upper layer. Due to this, surface current across the resistors is less as shown in **Figure 8(b)** which shows that EM wave passes through the resistors without any loss at the transmission window. At the out-of-band frequency regime, the non-resonating behaviour of the upper layer tank circuit leads to an extensive flow of surface current as shown in **Figure 8(a)** which leads to loss of EM wave at out-of-band (Absorption band) frequency regime. To get the above-said conditions, the values of chip resistors vary from *R=100* Ω to *R=200* Ω and the optimum result is found at *R=150* Ω. We can observe from **Figure 6** that chip resistors are responsible for only wideband absorption in out-of-band regime, the transmission behaviour is unaffected by the chip resistors.

VI. ABSORPTION/ TRANSMISSION PHENOMENA

The proposed rasorber's simulated absorption and transmission are illustrated in **Figure 7**. The proposed in-band rasorber operates within the frequency range of 2.8 to 10.0 GHz. The upper absorption band (80% absorption) is accomplished from 7.3 to 10.0 GHz, while the lower absorption band (80% absorption) occurs from 2.8 to 5.2 GHz. Near 5.93 GHz, the transmission window is identified as having an insertion loss of 1.10 dB, which is situated between the absorption bands.

The absorption and transmission phenomena of the rasorber depend on the different filtering action of the top and bottom layers. The upper layer is responsible for the absorption of EM waves in the out-of-band frequency regime

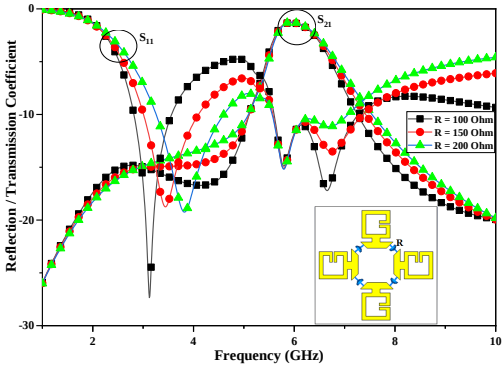

FIGURE 6: Reflection and transmission coefficient of the proposed Rasorber for different values of chip resistance.

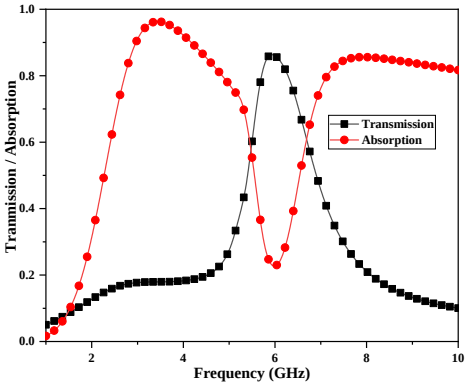

FIGURE 7: Simulated Absorptivity and Transmittivity for the proposed Rasorber.

and the bottom layer helps to get a transmission window between two absorption bands.

The proper impedance matching has been done between free space and proposed rasorber to enter the EM waves into the top layer of the rasorber. The top layer is realized by a parallel $L_1 - C_1$ tank circuit in series with R-L circuit. In the in-band frequency regime, the parallel $L_1 - C_1$ resonant circuit resonate leads to an impedance of infinity, which restricts the surface current across the resistors as shown in **Figure 8(b)** that shows the EM waves pass through the top layer unaffected with little insertion loss due to the finite loss tangent of the dielectric substrate. A circular slot has been cut in the lower layer which behaves as a band-pass filter to resonate the same frequency as the top layer as shown in **Figure 8**(d), the surface current density at the slot is high, which excite the slot and bottom layer act as a transparent window at the resonant frequency at around 5.93 GHz.

At the out-of-band frequency regime, Figure 8 (a, c) shows antiparallel current flows at the frequency of 3.0 GHz. As a result, a current loop is started, which creates a magnetic resonance and adjusts the permeability of the structure so that its impedance is equal to that of free space. Electric

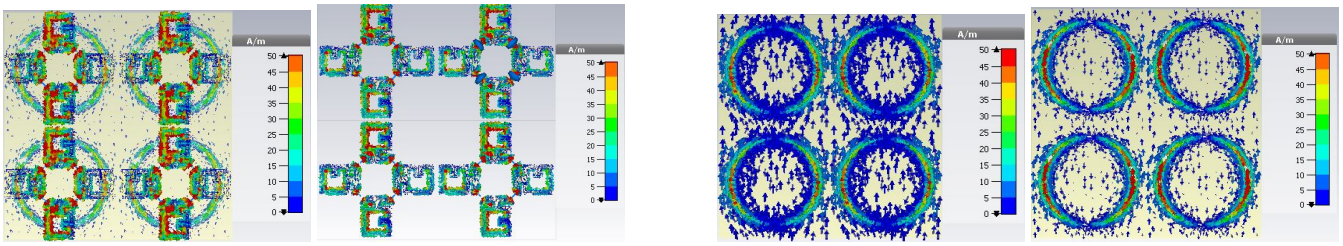

(a) (b) (c) (d)

FIGURE 8: Simulated surface current density of the proposed Rasorber at the top and bottom FSS (a,c) at 3.0 GHz (b,d) 5.93 GHz.

resonance also happens at the out-of-band frequency regime due to which the permittivity of the structure is adjusted. Electric and magnetic resonance happen simultaneously to match the structure impedance to the free space impedance, maximising absorption in the out-of-band frequency regime. Absorption phenomena can also be understood by the electrical equivalent circuit of the structure as parallel $L_1 - C_1$ tank circuit of the top layer is non-resonating in nature due to which a large amount of surface current flows through the chip resistors as shown in **Figure 8(a)**, which shows chip resistors is also responsible for the absorption in the out-of-band frequency regime, rest of the signal reach to the bottom layer via air-gap and reflected towards the top layer as the bottom layer behaves as a ground plane for the out-of-band frequency regime and again reflected from the bottom layer, this phenomenon occurs repeatedly to trap the signal in the structure, while in this journey if some waves leaked from the top layer, the air-gap and other design parameters adjusted to get destructive interference with incidence signal at the top surface of the proposed structure.

VII. POLARIZATION-INSENSITIVE BEHAVIOR

A. NORMAL INCIDENCE RESULTS

In order to evaluate the polarization capabilities of the proposed rasorber, the direction of propagation of the electromagnetic wave remains constant while the electric and magnetic field axes undergo rotation at a step size of 30° along a distinct polarization angle (ϕ).

As illustrated in **Figure 9**, the symmetrical configuration of the rasorber ensures that incident electromagnetic waves (EM waves) interact uniformly with the structure at all angles (ϕ) of incidence. Consequently, the reflection and transmission coefficients remain constant across various polarization angles. Thus, the designed rasorber is insensitive to polarization.

B. OBLIQUE INCIDENCE RESULTS

Equations (2) and (3) define the reflection coefficients for the TE polarization ($\Gamma_\perp$) and the TM polarization ($\Gamma_\parallel$) under the oblique incidence angle [29]:

$$\Gamma_\perp(\omega) = \frac{Z(\omega)cos(\theta_i) - Z_o cos(\theta_t)}{Z(\omega)cos(\theta_i) + Z_o cos(\theta_t)} \tag{2}$$

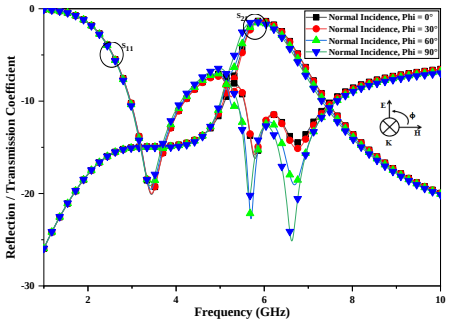

FIGURE 9: Simulated Reflection and Transmission coefficient for the proposed Rasorber for different polarization angles.

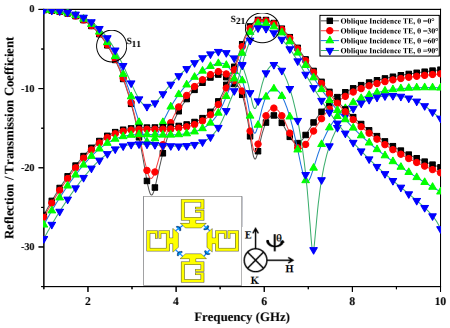

FIGURE 10: Simulated Reflection and Transmission coefficient of the proposed Rasorber for TE Polarization under oblique incidence.

$$\Gamma_\parallel(\omega) = \frac{Z(\omega)cos(\theta_i) - Z_o cos(\theta_t)}{Z(\omega)cos(\theta_i) + Z_o cos(\theta_t)} \tag{3}$$

Where θ_i,θ_t,$Z(\omega)$ and Z_o represent the angle of incidence, angle of transmission, impedance of the rasorber and free space impedance respectively.

As demonstrated by **equations 2** and **3**, the reflection coefficient is subject to variation based on the incident angle. **Figure 10** and **11** illustrate the variation in the reflection and transmission coefficients for a variety of incident angles (θ_i) under electromagnetic waves with TE and TM polarisations. The magnetic field direction and electromagnetic wave

TABLE 1: Experimental and simulation results of the proposed rasorber.

Simulated Rasorber				Measured Rasorber			
Reflection Coefficient		Transmission Coefficient		Reflection Coefficient		Transmission Coefficient	
Absorption	BW	Transmission window	IL	Absorption	BW	Transmission window	IL
More than 80%	2.8 to 10.0 GHz 7.2 GHz	5.93 GHz	1.1 dB	More than 80%	2.6 GHz to 9.7 GHz 7.1GHz	5.91 GHz	1.2 dB

TABLE 2: Comparison of the proposed rasorber with already published articles.

Design	Design Charact-eristics & Material	Periodicity ($\lambda_L \times \lambda_L$ (mm^2))	Transmission Peaks/ IL (dB)	Relative Absorption Bandwidth (RAB)	(Fractional Band-width)/ (Overall thickness)
[22]	A-T-A Different material for all layer (Expensive)	18 ×18/ (0.46×0.46)	8.8 GHz 1.0 dB	73.0 %, 24%	(113%) / (0.28λ)
[23]	A-T-A,$\epsilon_r = 3$ (Rogers 4230) (Expensive)	24×24/ 0.22×0.22	6.1 GHz/ 0.29 dB	91.40%, 31.90%	(112.4%) / (0.25λ)
[24]	A-T-A, FR4 $\tan\delta = 0.025$ (Low Cost)	26×26/ 0.43×0.43	3.68 GHz/ 1.28 dB	36.90%, 15.38%	(98.29%) / (0.18λ)
[25]	A-T-A, F4BM $\tan\delta = 0.0007$ (Expensive)	20×20/ 0.12×0.12	5.74 GHz, 0.25 dB	64%, 23%	(130%) / (0.25λ)
[26]	A-T-A Rogers 4350B $\tan\delta$=0.0037 (Expensive)	15×15/ 0.24×0.24	10 GHz, 0.2dB	66% 34%	(105%) / (0.25λ)
[27]	A-T-A FR4 $\tan\delta$=0.02 (Low Cost)	25×25/ 0.38×0.38	4.3 GHz, 0.81dB	68.4% 40%	(114.7%) / (0.20λ)
[28]	A-T-A FR4 $\tan\delta$=0.025 (Low Cost)	14.6×14.6/ 0.48×0.48	10.80 GHz, 1.0 dB	54.70% 14.1%	(96.10%) (0.186λ)
This Work	A-T-A FR4 $\tan\delta = 0.025$ Low Cost	15×15/ 0.12×0.12	5.93 GHz, 1.1 dB	57.14 %, 35.29 %	(113%) (0.18λ)

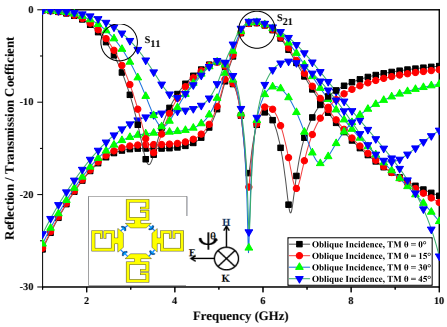

FIGURE 11: Simulated Reflection and Transmission coefficient of the proposed Rasorber for TM Polarization under oblique incidence.

propagation direction rotate at various incidence angles in TE polarisation, as illustrated in **Figure 10**, but the E-field direction remains constant.

In TM polarisation, the electric field direction and electromagnetic wave propagation direction both rotate at varying incidence angles; however, the H-field direction remains constant.

According to **Figure 10**, the reflection coefficient in the upper and lower band decreases slightly with an increase in the angle of incidence by a step of 15° but it remains more than 80% for the said frequency range up to 45°. The transmission window remains stable up to an incidence angle of 45° with a slight decrease in the insertion loss. In the case of TM polarization, while increasing the angle of incidence the absorption in the upper band increasing and it remains more than 80% in the lower band also up to 45°. The transmission coefficient is stable up to 45° with a slight decrease in insertion loss, shown in **Figure 11**.

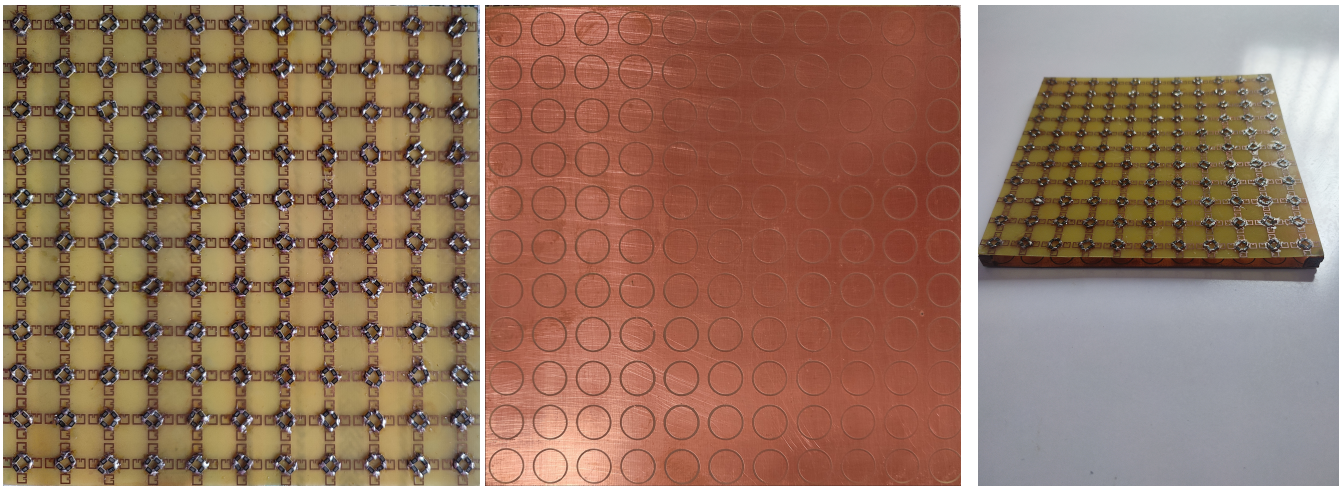

(a) (b) (c)

FIGURE 12: Fabricated proposed Rasorber prototype (a) Top layer (b) Bottom layer (c) Side view.

(a) (b)

FIGURE 13: Enlarged view of unit cell of the fabricated Rasorber (a) Top layer (b) Bottom layer.

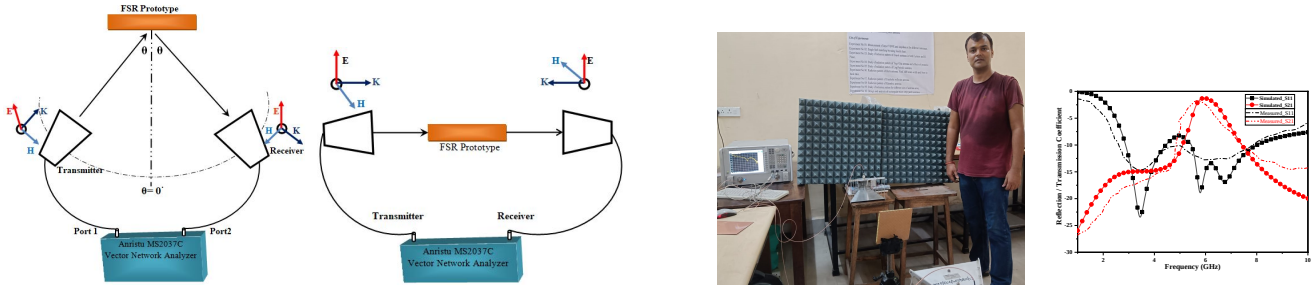

(a) (b) (c) (d)

FIGURE 14: Schematic diagram of the measurement setup for (a) Reflection Coefficient (b) Transmission Coefficient (c) Experimental setup for the measurement (d) Comparison between simulated and measurement results of the proposed Rasorber.

The air-space separating the upper and lower FSS functions as a transmission line, and its length is sensitive to oblique incidence; consequently, oblique incidence alters the overall input impedance of the transmission line, which in turn affects the rasorber's reflection and transmission coefficients.

VIII. PROTOTYPE FABRICATION AND VALIDATION

To validate the proposed rasorber, we have fabricated the top and bottom layer separately using PCB (Printed circuit board) technology and mounted the chip resistors on the top layer using soldering then assembled them for measurement, the top and bottom layers are separated using foam with refractive index near to air. The substrate for both layers was

1.0 mm thick FR4.

A photograph of the fabricated design is shown in **Figure 12**. **Figure 13 (a)** and **(b)** illustrate the enlarged views of the top and bottom layer fabricated samples, respectively. The semianechoic chamber was used to measure the fabricated sample of the rasorber. For this, we have used two 2-18 GHz horn antennas to send and receive electromagnetic waves which are connected to the Anristu MS2037C Vector Network Analyzer. To measure the reflection coefficient, two identical horn antennas are kept side by side in the same polarization; the absorber is kept between two horn antennas to minimize the effect of coupling. To remove the unwanted clutter a copper is kept at a distance more than $\frac{2D^2}{\lambda}$ in the far field region and the reflection coefficient is measured after that proposed rasorber is kept at the same distance and the actual reflection coefficient will be the difference between them.

The fabricated rasorber was positioned linearly between the two antennas to measure the transmission coefficient, as illustrated in **Figure 14(b)**. The normalisation was conducted with the unobstructed space or no obstruction between the two antennas. **Figure 14(a,b)** illustrates the measurement setup for reflection and transmission coefficient while **Figure 14(d)** shows the comparison between simulated and measured results. The measured results show more than 80% absorption from 2.6 GHz to 9.7 GHz with 1.2 dB insertion loss with a slight left shift of transmission plot, which is tabulated in **Table 1**. The plot demonstrates that the simulated and measured responses are in excellent agreement. The sample is offered support by the foam, which serves as a spacer.

Table 2 summarises the comparisons between the proposed meta-material rasorber and other related rasorbers that are currently available in the literature. The table illustrates that the proposed rasorber offers minimal thickness, high fractional bandwidth and high relative bandwidth on the right side of the absorption spectra. Additionally, it exhibits a reasonable periodicity and is cost-effective. The comparison table indicates that certain rasorbers exhibit minimal insertion loss; however, this is due to their higher periodicity and costly manufacturing costs.

IX. CONCLUSION

A compact rasorber is constructed with two layers. The upper layer comprises a modified split ring resonator affixed with lumped resistors to achieve broadband absorption, whereas the lower layer includes a circular slotted design to create a transmission window between two absorption bands. The design demonstrates a broad absorption band ranging from 2.8 to 10.0 GHz, with a lower absorption band from 2.8 to 5.2 GHz and an upper absorption band from 7.3 to 10.0 GHz, achieving a high fractional bandwidth of 113% within the absorption band, a broad transmission window with a -3dB bandwidth is expanded from 5.5 to 6.5 GHz, exhibiting a minimal insertion loss of only 1.10 dB, despite the dielectric substrate being a lossy FR4 material at approximately 5.93 GHz. The design structure is polarization-insensitive owing to its symmetrical configuration and maintains angular stability up to 45° for both TE and TM polarizations. The proposed rasorber is constructed utilizing PCB technology and validated in a semi-anechoic chamber, with the experimental results fully consistent with the simulated outcomes.

The proposed design features a broad transmission window, high fractional bandwidth, cost-effectiveness, accessibility through the use of inexpensive materials for manufacture, polarization insensitivity, angular stability, and a simple design. Our proposed rasorber has the potential to be utilized in electromagnetic compatibility applications to protect devices against electromagnetic radiation, including microwaves and radio waves. Furthermore, employing a rasorber as a superstrate antenna helps diminish RCS.

REFERENCES

[1] F. Costa and A. Monorchio, "A frequency selective radome with wideband absorbing properties," IEEE transactions on antennas and propagation, vol. 60, no. 6, pp. 2740–2747, 2012.

[2] H. Chen, X. Hou, and L. Deng, "Design of frequency-selective surfaces radome for a planar slotted waveguide antenna," IEEE Antennas and Wireless Propagation Letters, vol. 8, pp. 1231–1233, 2009.

[3] H. Zhou, S. Qu, B. Lin, J. Wang, H. Ma, Z. Xu, W. Peng, and P. Bai, "Filter-antenna consisting of conical fss radome and monopole antenna," IEEE Transactions on Antennas and Propagation, vol. 60, no. 6, pp. 3040–3045, 2012.

[4] P. Gurrala, S. Oren, P. Liu, J. Song, and L. Dong, "Fully conformal square-patch frequency-selective surface toward wearable electromagnetic shielding," IEEE Antennas and Wireless Propagation Letters, vol. 16, pp. 2602–2605, 2017.

[5] G. Chaitanya, P. Peshwe, S. Ghosh, and A. Kothari, "Miniaturized reconfigurable three dimensional printed frequency selective surface based microwave absorbers," Electromagnetics, vol. 44, no. 2-3, pp. 170–185, 2024.

[6] Z. Sun, Q. Chen, M. Guo, and Y. Fu, "Low-rcs reflectarray antenna based on frequency selective rasorber," IEEE Antennas and Wireless Propagation Letters, vol. 18, no. 4, pp. 693–697, 2019.

[7] Q. Chen, D. Sang, M. Guo, and Y. Fu, "Frequency-selective rasorber with interabsorption band transparent window and interdigital resonator," IEEE Transactions on Antennas and Propagation, vol. 66, no. 8, pp. 4105–4114, 2018.

[8] B. Li and Z. Shen, "Wideband 3d frequency selective rasorber," IEEE Transactions on Antennas and Propagation, vol. 62, no. 12, pp. 6536–6541, 2014.

[9] P. Munaga, S. Ghosh, S. Bhattacharyya, D. Chaurasiya, and K. V. Srivastava, "An ultra-thin dual-band polarization-independent metamaterial absorber for emi/emc applications," in 2015 9th European conference on antennas and propagation (EuCAP). IEEE, 2015, pp. 1–4.

[10] S. Ghosh, S. Bhattacharyya, Y. Kaiprath, D. Chaurasiya, and K. V. Srivastava, "Triple-band polarization-independent metamaterial absorber using destructive interference," in 2015 European Microwave Conference (EuMC). IEEE, 2015, pp. 335–338.

[11] R. A. Shelby, D. R. Smith, and S. Schultz, "Experimental verification of a negative index of refraction," science, vol. 292, no. 5514, pp. 77–79, 2001.

[12] Y. Cheng, X. S. Mao, C. Wu, L. Wu, and R. Gong, "Infrared nonplanar plasmonic perfect absorber for enhanced sensitive refractive index sensing," Optical Materials, vol. 53, pp. 195–200, 2016.

[13] D. Singh and V. M. Srivastava, "An analysis of rcs for dual-band slotted patch antenna with a thin dielectric using shorted stubs metamaterial absorber," AEU-International Journal of Electronics and Communications, vol. 90, pp. 53–62, 2018.

[14] B. Kumari, A. Kumar, P. Kumar, and M. Singh, "Polarization independent ultra-wideband meta-material absorber using conductive ink resonator," Journal of Telecommunications and Information Technology, no. 1, pp. 39–45, 2024.

[15] A. Kumar and J. Ghosh, "Polarization-independent wideband metamaterial absorber based on resistor-loaded hexagonal ring resonators,"

Journal of Electromagnetic Waves and Applications, vol. 38, no. 2, pp. 264–281, 2024.
[16] P. Ranjan, A. Choubey, S. K. Mahto, R. Sinha, and C. Barde, "A novel ultrathin wideband metamaterial absorber for x-band applications," Journal of Electromagnetic Waves and Applications, vol. 33, no. 17, pp. 2341–2353, 2019.
[17] P. Ranjan, C. Barde, A. Choubey, R. Sinha, and S. K. Mahto, "Wide band polarization insensitive metamaterial absorber using lumped resistors," SN Applied Sciences, vol. 2, no. 6, p. 1061, 2020.
[18] A. Varuna, S. Ghosh, and K. V. Srivastava, "An ultra thin polarization insensitive and angularly stable miniaturized frequency selective surface," Microwave and Optical Technology Letters, vol. 58, no. 11, pp. 2713–2717, 2016.
[19] B. Yi, P. Liu, G. Li, and Y. Dong, "Design of miniaturized and ultrathin absorptive/transmissive radome with wideband absorbing property," Microwave and Optical Technology Letters, vol. 58, no. 8, pp. 1870–1875, 2016.
[20] Q. Chen, L. Chen, J. Bai, and Y. Fu, "Design of absorptive frequency selective surface with good transmission at high frequency," Electronics Letters, vol. 51, no. 12, pp. 885–886, 2015.
[21] G. Sen, A. Sharma, S. Ghosh, and S. Das, "A wide inter-absorption dual-transmission dual-polarized frequency selective rasorber based on srrs," Electromagnetics, vol. 42, no. 5, pp. 348–358, 2022.
[22] H. Ye, W. Dai, X. Chen, H. Zhang, S. Bie, and J. Jiang, "High-selectivity frequency-selective rasorber based on low-profile bandpass filter," IEEE Antennas and Wireless Propagation Letters, vol. 20, no. 2, pp. 150–154, 2020.
[23] H. Huang and Z. Shen, "Absorptive frequency-selective transmission structure with square-loop hybrid resonator," IEEE Antennas and Wireless Propagation Letters, vol. 16, pp. 3212–3215, 2017.
[24] Y. Han, W. Che, X. Xiu, W. Yang, and C. Christopoulos, "Switchable low-profile broadband frequency-selective rasorber/absorber based on slot arrays," IEEE Transactions on Antennas and Propagation, vol. 65, no. 12, pp. 6998–7008, 2017.
[25] X. Zhang, W. Wu, Y. Ma, C. Wang, C. Li, and N. Yuan, "Design dual-polarization frequency selective rasorber using split ring resonators," IEEE Access, vol. 7, pp. 101 139–101 146, 2019.
[26] Q. Chen, D. Sang, M. Guo, and Y. Fu, "Frequency-selective rasorber with interabsorption band transparent window and interdigital resonator," IEEE Transactions on Antennas and Propagation, vol. 66, no. 8, pp. 4105–4114, 2018.
[27] A. Malekara, A. Khalilzadegan, C. Ghobadi, and J. Nourinia, "Wide-angle, dual-polarized frequency selective rasorber based on the electric field coupled resonator using characteristic mode analysis," Journal of Applied Physics, vol. 133, no. 16, 2023.
[28] X. Huang, Y. Ma, X. Li, L. Guo, and H. Yang, "Design of a frequency selective rasorber based on a band-patterned octagonal ring," Materials, vol. 16, no. 5, p. 1960, 2023.
[29] G. Sen, S. Das, and S. Ghosh, "Polarization-insensitive dual-band frequency selective rasorber based on concentric srrs," in 2020 International Symposium on Antennas and Propagation (ISAP). IEEE, 2021, pp. 263–264.